TECHNICAL PAPER

Effects of valve opening on direct water hammer pressure characteristics in PMMA pipelines

Xiaoying Zhang[1,2] · Shaokang Bian[1,2] · Hui Wang[3,4] · Xuanwen Jia[3,4] · Chuan Wang[3,4] 🔟

Abstract

In recent years, the application of viscoelastic pipelines in water supply engineering has become increasingly common. In pipes with viscoelasticity, the viscoelasticity of the pipe wall will attenuate the pressure wave as it propagates. Elastic materials have a different relationship between stress and strain than elastic materials. Whether the direct water hammer is generated by rapidly closing the valve under different valve initial opening degree from the transient elastic flow theory needs to be investigated in depth, as the deformation comprises instantaneous and delayed deformation components. A series of experiments is conducted in this paper to study the direct water hammer pressure generated in the polymethyl methacrylate (PMMA) pipeline when the valve initial opening degree is 100 and 30% at different flow velocities and obtains the effect of valve initial opening degree on the change in the direct water hammer pressure in the viscoelastic pipeline. The three-dimensional numerical simulation of the flow field near the valve was performed by using ANSYS-FLUENT. The results show that the value of the direct pressure of the water hammer in PMMA pipes is larger than that in Joukowsky formula, and all exceed the theoretical pressure value at the first wave peak. The variation in the valve closing time and the initial opening degree has an effect on the magnitude of the direct water hammer pressure in PMMA pipelines. Under the condition of 6 different flow rates with the same valve closure time, the direct pressure of the water hammer generated by 30% valve initial opening is larger than that generated by 100% valve initial opening with fast valve closure, and the pressure difference is between 5.62 and 10.48%. The obtained results via numerical simulation show the turbulent flow pattern near the valve and the large average flow velocity under a small valve opening degree. This phenomenon leads to the generation of a large direct water hammer pressure via the sudden closing of the valve.

Keywords Viscoelastic pipeline · Direct water hammer · Valve opening degree · Experimental study · Numerical simulation

1 Introduction

Nowadays, with the development of economy and the accelerating process of globalization, the construction of long-distance pipeline transportation projects is flourishing. In the context of the great development of marine resources, pipeline transportation is widely used in ocean engineering, which can provide a relatively economical and safe transportation method for liquid resources such as oil and fresh water. With the development of material science, pipelines comprising organic polymer materials have been gradually applied to domestic and foreign engineering practice due to their advantages of low cost, light weight, and corrosion resistance. For example, PVC, PE, and HDPE are currently widely used in pipeline materials. Statistics indicate that 30% of pipelines in the USA comprise viscoelastic materials; approximately 35% of the metal piping has been replaced with plastic piping in water transmission lines [1].

Improper operation in long-distance pressurized water pipelines can induce substantial water hammer pressure,

Technical Editor: Erick Franklin.

✉ Chuan Wang
  wangchuan198710@126.com

1 College of Hydraulic and Civil Engineering, Xinjiang Agricultural University, Urumqi 830052, China

2 Xinjiang Key Laboratory of Hydraulic Engineering Security and Water Disasters Prevention, Urumqi 830052, China

3 International Shipping Research Institute, GongQing Institute of Science and Technology, Jiujiang 332020, China

4 College of Hydraulic Science and Engineering, Yangzhou University, Yangzhou 225009, China

which can seriously harm the entire pipeline system [2–6]. The frequent occurrence of water hammer accidents in viscoelastic pipelines is also a new issue that must be urgently solved. In the field of transient flow, scholars have conducted a considerable amount of research on the water hammer problem, which mainly established the mathematical model of the pressurized water pipeline to simulate the hydraulic transition process and investigated effective water hammer protection measures to ensure the safe operation of projects. Tran [7] studied the pressure transient caused by the closing of the air valve in the filling pipeline and proposed a filling rate method considering different factors of pipeline safety. Besharat et al. [8] conducted several experiments on the compressed air container, obtained the absorption effect of the device on the water hammer pressure, and analyzed the effects of the airbag size on the water hammer pressure. Miao et al. [9] proposed that the combined protection of the air tank and the downstream valve can effectively reduce the water hammer pressure and the air tank volume. Yang et al. [10] introduced a new formula and continuity equation for the calculation of water hammer wave velocity, which solved the unsatisfied constant flow condition problem by the continuity equation. Fu et al. [11] improved the calculation model of the two-fluid gas–liquid two-phase flow and successfully predicted the liquid column separation phenomenon in pipeline gas–liquid two-phase flow. Wang et al. [12] established the mathematical model of the air valve in the process of filling an empty pipeline with water and obtained the optimal air valve model. Chen et al. [13] used experimental method and numerical calculation to analyze the influence of the closing valve speed on the impact waveform of the water hammer. Roberts et al. [14] presented an experimental study involving a small-scale model device driving a piston crank mechanism to demonstrate that the operating principles behind hydraulic rams can also be adapted to provide renewable energy. Wang et al. [15] established a mathematical model of the transition process of the entire system, including the water pump, pipeline, and water hammer protection measures, by substituting the pressurized water delivery system for an energy conversion mechanism. Li et al. [16] proposed a pump-stop water hammer protection scheme, in which the air tank and the overpressure relief valve are jointly established. For the OAA load-shedding conditions of PSS, Wei et al. [17] revealed the mechanism for the extreme WHP in the TST through theoretical analyses, numerical simulations, and model experiments. Wang et al. [18] used MATLAB programming to simulate the water hammer and calculated and studied the water hammer pressure generated at the moment of valve closing. Zhang et al. [19] introduced the friction of long diversion tunnels into the traditional water hammer analytical method and derived a new series of analytical formulas for water hammer considering the friction of long diversion tunnels, a

formula for calculating the critical opening, and a formula for limiting the closure law based on the extreme value of water hammer at small openings. Li et al. [20] performed numerical simulations on water hammer protection of various types of air valves in pressurized pipelines. The research on water hammers is not limited to the above water pipelines, and the water hammer is crucial in the field of jet flow [21, 22] and pump [23, 24]. Therefore, the study of water hammers is of considerable importance. For the study of the hydraulic characteristics of viscoelastic pipelines, Triki A et al. [25, 26] investigated an in-line design strategy using short pipe sections with polymeric wall materials (HDPE and LDPE) to replace transient sensing zones in steel pipe. They found that the newly proposed technique can effectively reduce the water hammer pressure and circumferential stresses through experimental comparison, showing that the technique can effectively mitigate the severe impacts of the water hammer on pipes and provide novel ideas for the safe design of water distribution systems. Wang et al. [27] focused on analyzing the pressure variation trend of the viscoelastic pipelines in the electrical circuit model, deduced the calculation formula for the propagation velocity of pressure waves, and obtained several methods of the actual propagation velocity through the experimental curve. Zhang et al. [28] focused on the tank–pipeline–valve system and studied the water hammer characteristics of elastic and viscoelastic pipelines and found that the pulsating pressure head of viscoelastic pipelines rapidly decays with time. Bergant et al. [29] investigated the effect of pipe wall viscoelasticity on water hammer pressure by performing water hammer tests in a tank pipe valve system consisting of a polyvinyl chloride (PVC) main pipe and two short steel pipes, and the results have shown that pipes with viscoelastic materials have an attenuating effect on the pressure of the water hammer, in addition to the flow–solid coupling, the nonlinear viscoelastic effects of the pipe wall vibration, and other factors that may affect the water hammer pressure of the viscoelastic pipes. Gally et al. [30] proposed the introduction of viscoelastic terms in the continuity equation to describe the delayed strain in viscoelastic pipelines. Covas et al. [31, 32] experimentally measured the creep function of the viscoelastic pipe to investigate the effect of wall shear stress on the transient flow in this pipeline and proved that stress conditions to which the pipeline is subjected vary depending on the wall constraint. Soares et al. [33] performed experiments on PVC pipes through experiment and simulation. Under transient flow conditions, the viscoelastic behavior of PVC pipes has a significant effect on hydraulic transients. Therefore, the viscoelastic properties of pipe walls must be considered when designing and analyzing transient hydraulic processes. Ghidaoui et al. [34] calculated the effects of pipeline viscoelasticity on the attenuation of transient flow pressure fluctuations according to the

acceleration weighting function. They found the large effect of viscoelasticity on pressure fluctuations as the fluctuation time extended. Keramat et al. [35, 36] investigated the Poisson's ratio of viscoelastic pipelines with time and obtained the factors affecting the problem of axial vibration response characteristics of viscoelastic pipelines. Keramat et al. [37] studied the effect of fluid–structure coupling on the water hammer pressure in PE pipes through water hammer testing in viscoelastic pipes with a multi-axial bearing. Results have shown that the stiffness and location of the support structure affect the pressure distribution profile. However, structural boundary features affect the transient pressure spectrum, and the results of the tests have important implications for piping system design and fault detection. A viscoelastic Joukowsky formulation was proposed by Keramat A et al. [38], and the applicability of the proposed formulation was tested using two polyethylene pipe cases, and the results have shown that the method is highly effective for sufficiently long pipes with complete creep during the one-half cycle of transient flow and is more efficient and easier to implement than the classical technique of inverse transient analysis. The effect of fast valve closure was studied by Meniconi et al. [39], viscoelasticity and unsteady friction on the transient behavior of pressurized pipelines as shown in Fig. 4 of the paper, and assessed the effect of the initial Reynolds number and the local loss coefficient on the water hammer pressure through numerical simulations and physical model tests. Jeno et al. [40] conducted numerical simulations of a butterfly valve to elucidate the relationship between the flow field structure and the flow characteristics inside the valve. Zhang Y et al. [41] investigated the effect of a water hammer in pipelines caused by switching pumps and closing valves and explored the effect of the air chamber capacity on the water hammer pressure using the VOF model, suggesting that the air must be efficiently vented prior to pump and valve operation. The effect of different ballvalve closure times on water hammer pressure variation was investigated by the CFD software by Han Y et al. [42], and numerical simulation results have shown that the length of the valve closure time affects the vortex core motion and pressure vibration, and prolonging the closing time of the valve can effectively reduce the maximum pressure of the water hammer, which can be used as a reference for water hammer protection during ball valve closure in pipeline systems.

In recent years, most researchers have obtained more abundant results on transient flow problems in elastic pipes, and for plastic pipes PE, PVC, PP, PMMA, and other viscoelastic pipes of this type, if we continue to use classical transient flow theory for numerical simulation studies, the results will have some deviation [35, 43]. Numerical and experimental investigations have been carried out for viscoelastic responses in either plastic or polymeric pipelines [26, 44, 45]. The experimental results showed that the strain rate of the viscoelastic pipe was much higher than that of the elastic pipe, and the viscoelastic conduit may be able to withstand a more severe pressure rise than the elastic conduit.

They also introduced many solutions that have been applied to practical engineering to reduce water hammer pressure. However, the viscoelastic effect of the pipeline is rarely considered in the design scheme for the safe operation of the currently used viscoelastic pipeline water supply projects, such as PE、PVC、PMMA and PPR. This effect is only considered in the calculation of the wave speed and the lateral and axial strains of the pipe wall. The water hammer pressure still uses the transient flow theory of elastic pipelines as the basis for the design of water supply projects, and the calculation of the direct water hammer pressure is still performed using the Joukowsky formula. The viscoelasticity of viscoelastic pipes significantly influences the pressure responses and results in the classical Joukowsky pressure head not being valid for the entire half-period of the water hammer. Despite the fact that many researchers have introduced the Kelvin–Vogt model into the mathematical model of viscoelasticity and have considered a term in the continuity equation based on it, in addition, special mechanical tests have been carried out to measure the viscoelastic properties of the pipe wall material. In the aforementioned studies, only the material properties of the pipe were investigated. Covas, Pezzinga, Brunone et al. [31, 32, 46] have carried out extensive research on viscoelastic pipes, which provided the research basis for our paper. They mention that the main property of viscoelastic materials is that the strain response lags behind the applied stress. This behavior affects the pressure response during transient events by attenuating pressure fluctuations and increasing the dispersion of the pressure wavefront. Keramat, Tijsseling, Bergant et al. [38, 47] conducted many researches on the viscoelastic Joukowsky head (VJH) formula, which contributes to the study of water hammer in viscoelastic pipes. The objective of this paper was to measure the pressure of the direct water hammer generated inside a viscoelastic pipe such as PMMA and provide valuable experimental data which can be used to check the accuracy of the viscoelastic model.

If the elastic pipeline characteristics are used as the theoretical basis in the simulation research of the hydraulic transition process of the viscoelastic pipeline, then the possible accurate application of the results to the actual engineering must be further studied. If the research on the hydraulic transition process in the viscoelastic pipeline is insufficient and the actual project fails to meet the requirements of design and operation, then serious water hammer accidents will occur, resulting in major personal safety hazards and economic losses. With the development of pipeline technology, the impact factors taken into account during testing have become increasingly complex, and the transient flow

model requirements for viscoelastic pipelines have become increasingly stringent; there is a need for more accurate testing of the hydraulic transition process for viscoelastic pipelines in order to reflect real pipeline pressure fluctuations and thus accurately modify the model. In the theory of water hammer, the magnitude of direct water hammer is independent of the initial opening of the valve, i.e., the maximum value of direct water hammer pressure is fixed regardless of the initial opening of the valve; therefore, it is the culmination of this paper to explore whether the magnitude of the direct water hammer pressure generated by different valve apertures in PMMA pipelines is the same. Therefore, conducting in-depth experimental research on the variation law of water hammer pressure in viscoelastic pipelines and understanding the dynamic characteristics of viscoelastic pipeline materials for its practical application is of considerable importance.

2 Experimental device and measurement method

Figure 1a shows the device system, which comprises an upstream water tank, PMMA pipes, a midline butterfly valve, a flow regulating valve, and a downstream water tank. The actual layout of the pipeline is shown in Fig. 1b, in which the length of the experimental pipe is 44.37 m, the inner diameter of the pipe is 5 cm, and the wall thickness of the pipe is 1 cm. For PMMA pipe, its mechanical properties are similar to those of polyethylene plastic, with typical viscoelastic behavior [31, 32, 44], this paper will focus on PMMA pipe as a research object in addition to its own features of viscoelastic pipe, the primary reason for this is that PMMA piping has the characteristics of transparency, transparent PMMA can observe the flow conditions of the fluid in the pipe, easy to observe the water hammer generated in the process of the pipe if the state of separation of the liquid column, by observing if the pipe is producing gas, and the range of changes in flow rate is determined to avoid the flow of water into the pipe to produce a water hammer bridging the break. A midline butterfly valve is set at the end of the pipeline, which is 42.37 and 2.0 m away from the upstream and downstream water tanks, respectively. Direct water hammer is generated in the pipeline by manually closing the valve. Figure 1c shows the installed high-frequency dynamic pressure sensors 0.5 m away from the end of the pipeline and 2 m away from the front of the midline butterfly valve to measure water hammer pressure. An overflow plate is set in the upstream water tank to maintain the upstream water level, and a 90° triangular sharp-crested weir is set in the downstream tank to measure the flow in the pipeline. Buttresses are set at intervals of 1 m near the end valve

and 2–3 m in the first half of the pipeline. This experiment mainly studies the water hammer caused by the rapid closing of the valve under different flow velocities.

The flow velocity in the pipe is between 0.11 and 0.29 m/s after calculation to ensure the turbulent water flow in the pipe. This experiment uses a 90° triangular sharp-crested weir, ultrasonic flowmeter, and weighing method to measure the flow simultaneously to ensure the accuracy of flow measurement. The flow errors measured by the three methods are within $\pm 5\%$. The pressure sensor (GYG1405F) is a high-frequency high-precision dynamic pressure sensor with an accuracy level of 0.5% F.S and a frequency response of 20 kHz. The pressure of the water hammer was collected using the CrAs data monitoring and acquisition system shown in Fig. 1d. The water temperature tested before the experiment ranged from 13 to 15 °C. The experiments were conducted under the conditions of six flow velocities with the midline butterfly valve at 100 and 30% openings, as shown in Fig. 2. In addition, Fig. 3 illustrates the flow of this experimental study. The basic theory of the water hammer states that the direct water hammer phenomenon will occur in the pipeline when T_c, which is the closing time of the valve, is not more than $2L/a$. The direct water hammer is generated in the pipeline after calculation when $T_c \leq 120$ ms. Therefore, the closing time of the valve is set to be less than 120 ms under all working conditions in this experiment. At least 10 experiments of rapid closing of the valve are performed under each flow velocity condition: the first five valve closing operations are conducted at a high speed to verify that the experiment meets the repeatability of the test, and the last five valve closing operations are conducted at a slightly slower speed. These conditions meet the requirements of a direct water hammer to determine the effects of different valve closing times on the direct water hammer pressure.

3 Calculation model and boundary conditions

FLUENT is used to simulate numerically the steady flow of the midline butterfly valve with 30 and 100% openings. The analysis of the internal flow field distribution of the valve with different openings under various flow velocities further explained the effect of the bottom flow pattern on the direct water hammer pressure under different valve openings. The basic equations of computational fluid dynamics include mass and momentum conservation equations. The length of 4 m before and after the midline butterfly valve is selected in the calculation model. Figure 4 shows the 3D model of the butterfly valve with 100 and 30% openings. GAMBIT is used to
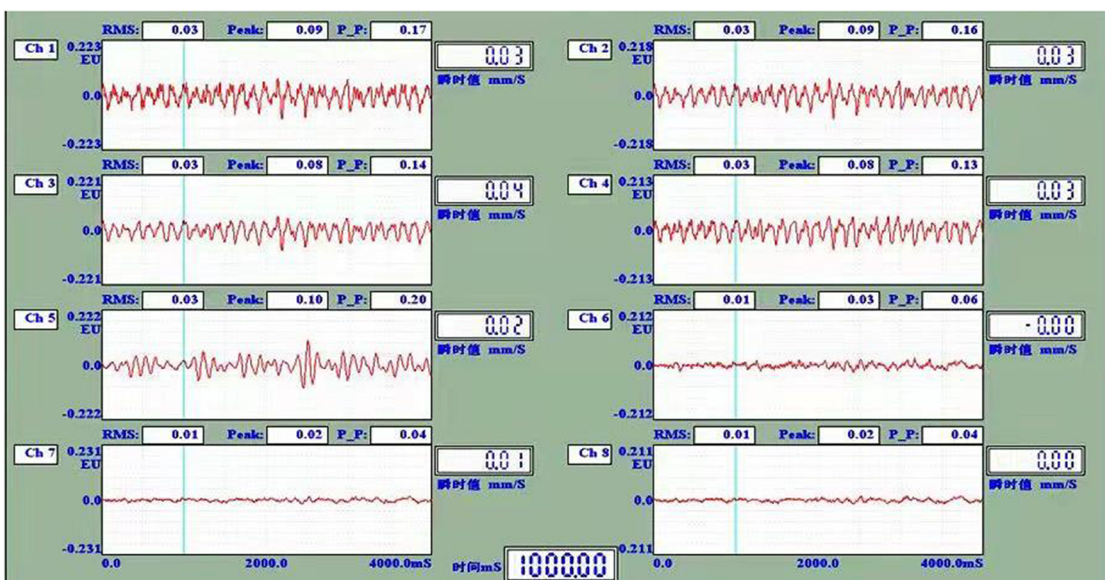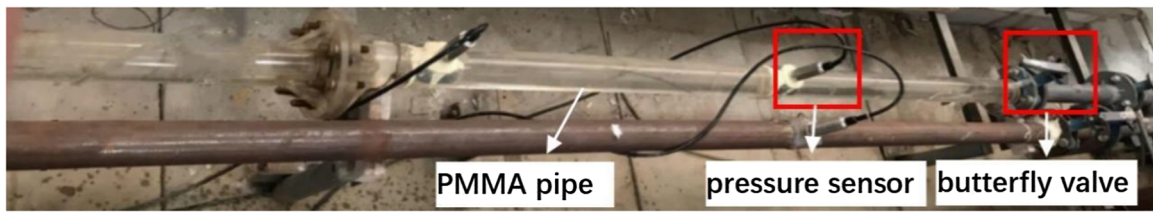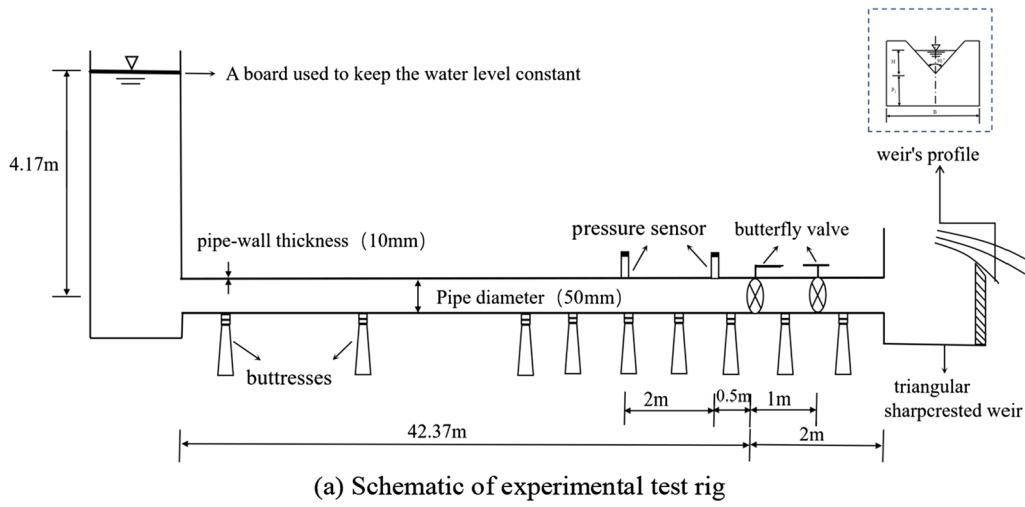
(a) Schematic of experimental test rig

(b) Actual layout of pipelines

(c) Pressure transducer

(d) Data acquisition interface of CrAs system

Fig. 1 Test device layout and acquisition equipment

Fig. 2 Butterfly valves with different opening degrees

(a) Butterfly valve at 30% opening

(b) Butterfly valve at 100% opening

Fill and vent the pipelines

↓

Calibrate measuring instruments

↓

Adjust to target flow

↓

Close valve quickly

↓

Collect and process date
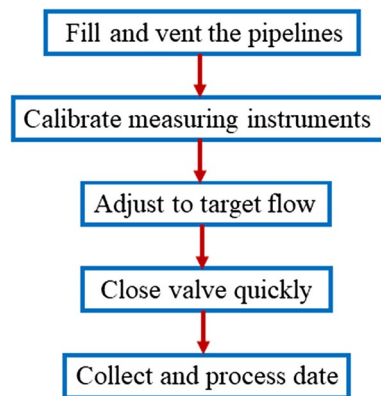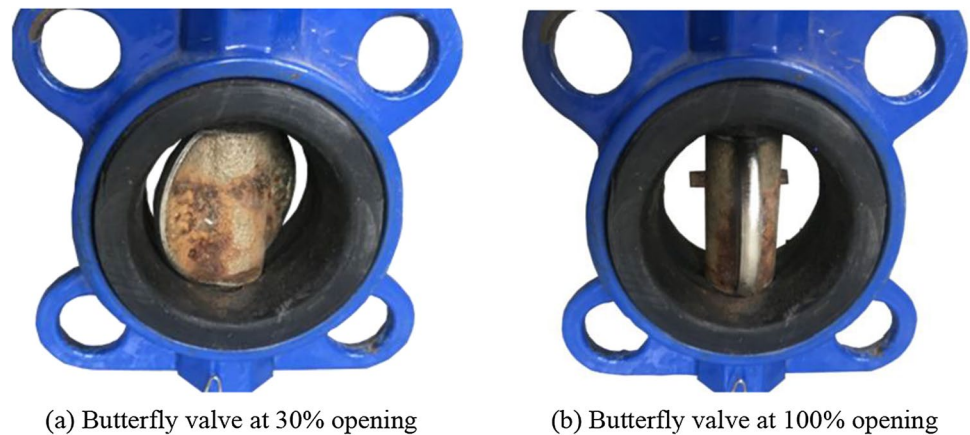
Fig. 3 Experimental procedures

establish the geometric model and mesh the butterfly valve, in which the *X*-axis direction and the origin are set as the flow direction of the fluid and the valve core, respectively. The SIMPLEC algorithm is also utilized in the calculation to solve the pressure and velocity: the inlet of the pipeline adopts a velocity boundary whose magnitudes are similar to the six velocity magnitudes in the experiment, and the outlet of the pipeline adopts a free outflow boundary. The mesh division adopts highly adaptive unstructured tetrahedral meshes, and the mesh number of the DN50 butterfly valve under different openings is 190,083 ~ 210,524.

4 Results and discussion

4.1 Effects of valve closing time on direct water hammer pressure

Figures 5 and 6, respectively, compare the experimental results of the direct water hammer pressure with those calculated by Eq. 1, which is the theoretical formula of transient flow. Three groups were randomly selected from the five groups of experimental data obtained under the same working conditions to illustrate the variation diagram of direct water hammer pressure under the condition of 100% valve opening, as shown in Fig. 5. This figure reveals that the three extracted groups of experimental data are consistent, thus demonstrating that the experiment meets the repeatability requirements.

$$\Delta H = -\frac{a}{g}\Delta V, \tag{1}$$

where ΔH is the increase in the water hammer pressure in m, a is the wave velocity in m/s, and ΔV is the variation in flow velocity in m/s.

Figure 5 shows that the measured value of direct water hammer pressure at each flow velocity is larger than the theoretical value of water hammer pressure calculated by Eq. 1. The maximum pressure generated by the closing valve in groups 1 to 3 and the initial head of the upstream tank is 12.64, 12.73, 12.73, and 4.16 m when *V*, which is the flow
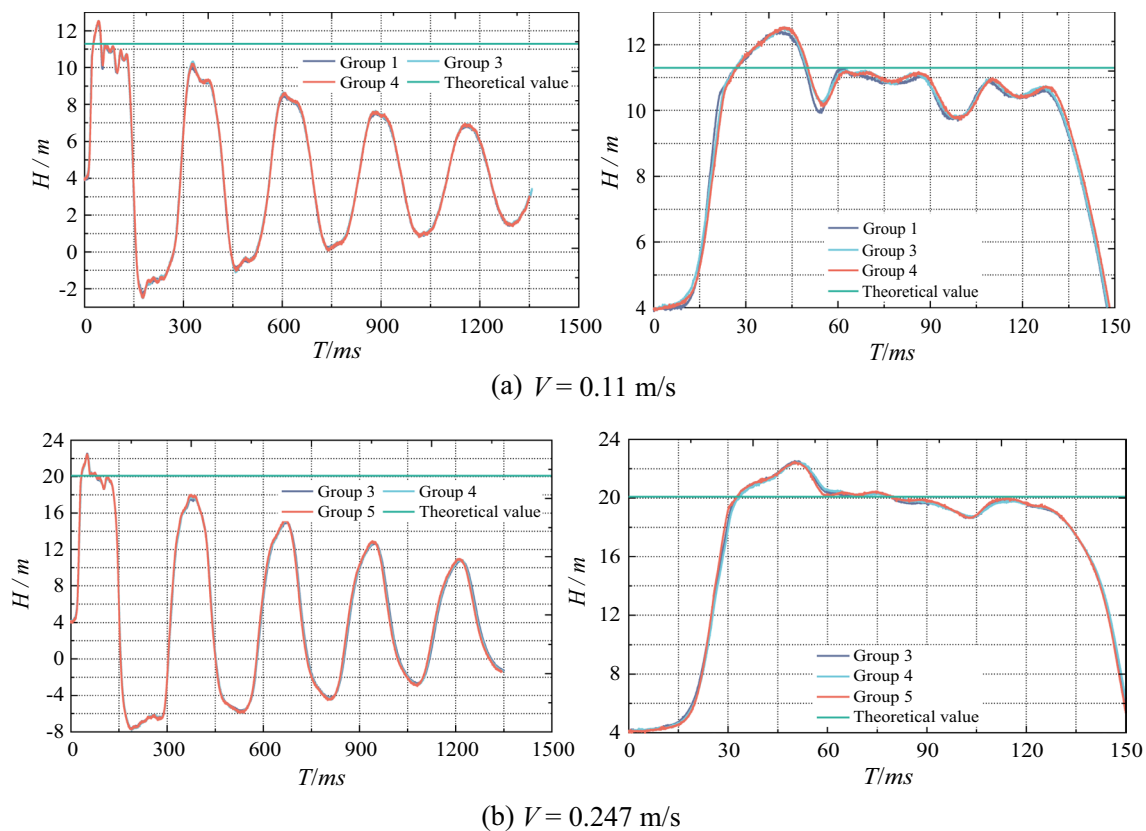
Fig. 4 Three-dimensional model of the butterfly valve at different openings

(a) Butterfly valve at 30% opening

(b) Butterfly valve at 100% opening

(a) $V = 0.11$ m/s

(b) $V = 0.247$ m/s

Fig. 5 Variation in direct water hammer pressure at 100% valve opening at different flow velocities

velocity, is equal to 0.11 m/s. Therefore, ΔH, which is the boost value of the water hammer, can be calculated. The boost values of the water hammer obtained from the three valve closing experiments are 8.48, 8.57, and 8.57 m. The theoretical boost value is 7.14 m, which is calculated by Eq. 1 and is 1.43 m lower than the measured value, which is approximately 20.03% low. The theoretical boost value is equal to 16.04 m and the measured boost values are 18.48, 18.39, and 18.41 m when $V = 0.247$ m/s. By contrast, the maximum boost value obtained by the three experiments is 2.44 m larger than the theoretical value, which is approximately 15.21% large, when $V = 0.247$ m/s.

Figure 6 shows the change in the measured direct water hammer pressure at different flow velocities when the initial valve opening is 30%. The figure reveals that the measured direct water hammer pressure at each flow velocity is also larger than the theoretical value, which is the same conclusion as when the initial opening is 100%. Figure 6a shows that one of the measured pressure boost values is equal to 11.80 m and the theoretical boost value is equal to 9.55 m when $V = 0.147$ m/s; thus, the measured boost is larger than the theoretical value of 2.25 m, which is approximately 23.61% large. The three other measured boost values exceeded the theoretical values by 23.61, 24.06, and 24.11%. Figure 6b shows that the three measured boost values exceeded the theoretical values (14.03 m) by 25.49, 26.68, and 24.49% when $V = 0.216$ m/s.

The relative values of closing times at different flow velocities at 100 and 30% openings are plotted against the increased percentage of direct water hammer pressure in Fig. 7 to analyze the effect of different closing times on the variation in direct water hammer pressure in viscoelastic pipes. Figure 7a reveals that the direct water hammer pressures at different flow velocities all exceed the theoretical values calculated by Eq. 1 when the valve opening is 100%. When $V = 0.147$ m/s, the variation range of T_t/T_c is 0.38–0.31 (the valve closing time is reduced from 46 to 37 ms) and the percentage exceeding $(H_t - H_c)/H_c$, which is the traditional value, increases from 11.62 to 21.04%. When $V = 0.183$ m/s, the range of T_t/T_c is 0.54–0.35 (the valve closing time is reduced from 65 to 42 ms) and $(H_t - H_c)/H_c$ is increased from 10.69% to 18.86%. When $V = 0.284$ m/s, the range of T_t/T_c is 0.65–0.35 (the valve closing time is reduced from 78 to 42 ms) and $(H_t - H_c)/H_c$ is increased from 2.49 to 17.19%. Figure 7b shows that the direct water hammer pressures at different flow velocities also exceed the theoretically calculated values when the valve opening is 30%. When $V = 0.11$ m/s, the variation range of
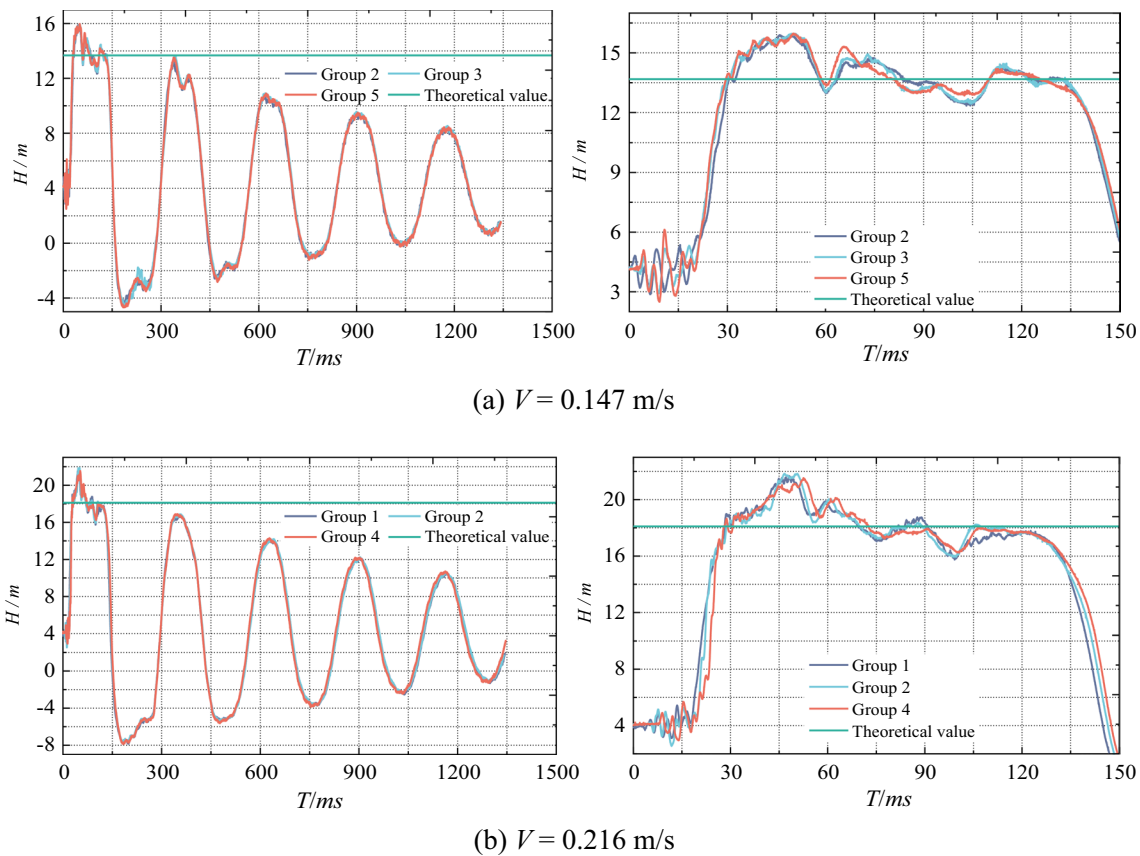
(a) $V = 0.147$ m/s

(b) $V = 0.216$ m/s

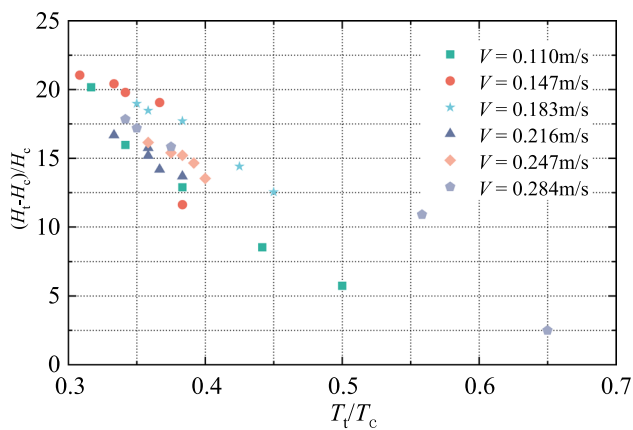**Fig. 6** Variation in direct water hammer pressure at 30% valve opening at different flow velocities

T_t/T_c is 0.41–0.33 (the valve closing time is reduced from 49 to 40 ms) and $(H_t - H_c)/H_c$ increases from 22.69 to 30.53%. When $V = 0.183$ m/s, the variation range of T_t/T_c is 0.45–0.33 (the valve closing time is reduced from 54 to 39 ms) and $(H_t - H_c)/H_c$ increases from 18.43 to 31.90%. When $V = 0.216$ m/s, the variation range of T_t/T_c is 0.43–0.33 (the valve closing time is reduced from 52 to 40 ms) and $(H_t - H_c) / H_c$ increases from 17.89 to 32.07%.

The above results show that the closing time of the valve has a substantial influence on the increase in the water hammer pressure in the viscoelastic pipeline, and the water hammer pressure rises with the decrease in the closing time of the valve. The above phenomenon is attributed to the viscous and elastic deformation mechanisms of the viscoelastic pipe. The viscoelastic pipe is relatively "soft," and the deflection of the pipe wall is large. Under the action of stress, the viscoelastic pipe will not only produce instantaneous strain similar to viscoelastic pipes but also generate some strain that lags behind the stress. The elastic modulus, wave velocity, and the direct water hammer pressure are all large when other variables are maintained.

Figure 8 shows the water hammer pressure generated by rapidly closing the valve at a certain flow velocity. The figure reveals that the pressure gradually increases at the beginning

of the valve closing and reaches the maximum value when the valve is completely closed. The elastic after-effects of viscoelastic pipes after valve closing induce stress from the PMMA pipeline without producing a corresponding strain, which results in a relatively large rigidity of the pipe and elastic modulus at this time. Thus, the wave velocity and the increase in water hammer pressure are large. Therefore, the actual measured direct water hammer pressure is larger than the theoretical value, which is calculated in Eq. 1. After the valve is closed for a period, a large strain occurs in the pipeline, the pressure wave begins to decay, the elastic modulus decreases relatively, and the wave velocity reduces, which eventually result in pressure reduction. The water hammer pressure does not change after recovering from a relatively large value to the theoretically calculated value when the strain reaches the maximum. Therefore, the wave of water hammer pressure first increases and then decreases rapidly and finally flattens. The pipeline does not react immediately due to the rapid closing of the valve. The "rigidity" of the pipe is relatively large under constant stress and small strain. As the elastic modulus increases, the wave velocity rises and the measured water hammer pressure also increases.

The above experimental results indicate that under 100 or 30% valve opening, the increase in water hammer pressure

(a) Butterfly valve at 100% opening
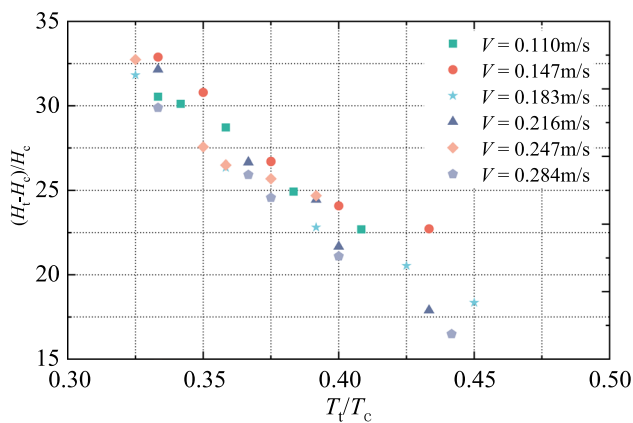
(b) Butterfly valve at 30% opening

Fig. 7 Relationship between the relative value of valve closing time and increase in direct water hammer pressure under different valve openings
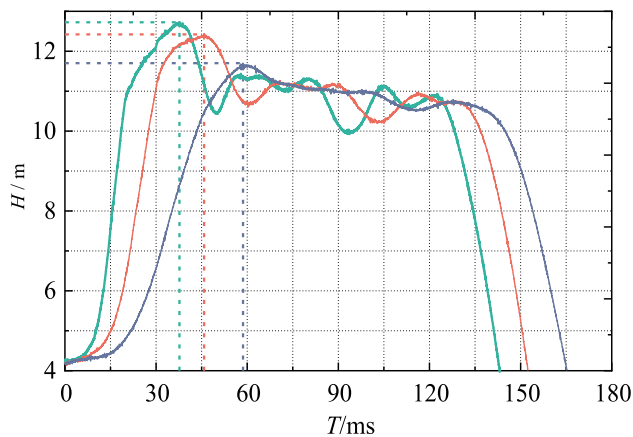

Fig. 8 Water hammer pressure generated by rapidly closing valve at a certain flow velocity

due to the rapid closing of the valve at each flow velocity far exceeds its theoretically calculated value. The increase in water hammer pressure generated at 100 and 30% valve openings, respectively, exceeded their corresponding theoretical values by 21.08 and 32.88%. The traditional theory of water hammer indicates that the increase in direct water hammer pressure is only related to the wave velocity in the pipe, the change in the flow velocity, and the acceleration of gravity; this phenomenon is unaffected by the closing time of the valve. However, the experiment found that a short valve closing time induces a high direct water hammer pressure. This finding further demonstrated that the formula of the direct water hammer did not match the measured direct water hammer pressure in the PMMA pipe, while that of direct water hammer pressure no longer applies to the calculation of direct water hammer pressure in elastic–viscoelastic pipes.

where T_t is the valve closing time measured in the experiment and T_c is the maximum time that the valve can be closed to ensure the occurrence of direct water hammer (its value is 120 ms). H_t is the water hammer pressure measured in the experiment, and H_c is the water hammer pressure calculated by Eq. 1.

4.2 Effects of initial valve opening on direct water hammer pressure

The direct water hammer pressure generated by valve closure when the initial valve opening is 100 and 30% under six different flow velocities was compared to analyze the influence of the initial valve opening on the direct water hammer pressure in the viscoelastic pipeline. Two experimental results with the same valve closing time were selected at each flow velocity for comparison, and the comparison results are shown in Fig. 9. Figure 9a reveals that when $V = 0.11$ m/s, the theoretically calculated pressure is 11.29 m, and the maximum pressure at 100% valve opening is 12.42 m, which exceeds the theoretical value by 10.0%. The maximum pressure at 30% valve opening is 13.12 m, which exceeds the theoretical value by 16.14 and is 8.38% higher than that at 100% valve opening. Figure 9b shows that when $V = 0.147$ m/s, the maximum pressures at 100% and 30% valve openings are, respectively, 15.61 and 16.81 m, which correspondingly exceed the theoretical value at 13.68 m by 10.0 and 22.94% (10.4% higher than that at 100% valve opening). Figure 9c demonstrates that when $V = 0.183$ m/s, the maximum pressure at 30% valve opening is 5.62% higher than that at 100% valve opening. Figure 9d shows that when $V = 0.216$ m/s, the maximum pressure at 30% valve opening is 10.48% higher than that at 100% valve opening. Figure 9e reveals that when $V = 0.247$ m/s, the maximum pressure at 30% valve opening is 8.84% higher than that at 100% valve opening. Figure 9f indicates that when $V = 0.284$ m/s, the maximum pressure at

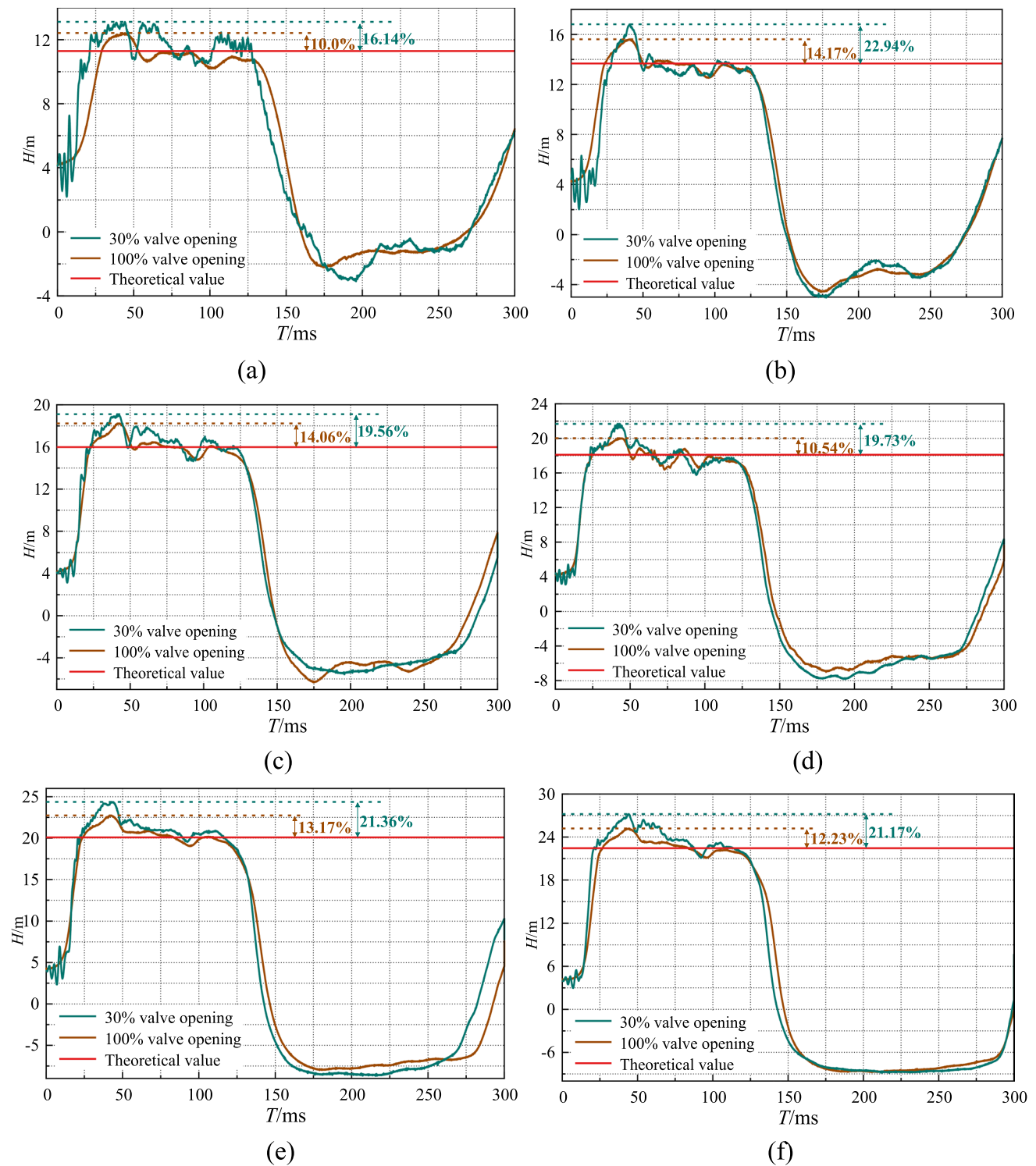(a)   (b)

(c)   (d)

(e)   (f)

Fig. 9 Comparison of pressures generated by different initial valve opening valves at various flow velocities

30% valve opening is 9.52% higher than that at 100% valve opening. The above comparison results show that the pressure at 30% valve opening is larger than that at 100% valve opening while that at 100% valve opening is larger than the

theoretically calculated pressure under similar valve closing times. In the traditional theory of direct water hammer, the water hammer pressure does not affect the initial opening of the valve and the direct water hammer pressure remains

the same regardless of the initial valve opening. However, the experimental results reveal that the direct water hammer pressure generated in viscoelastic pipes, such as PMMA, is related to the initial opening of the valve. A small initial opening of the valve leads to a high direct water hammer pressure.

4.3 Results and analysis of numerical simulation

A three-dimensional numerical simulation of the bottom flow pattern of the valve under different openings was conducted to analyze the reasons for different valve openings due to various increments in water hammer pressure. The flow velocities of the inlet are set similarly to those in the experiment, and the three-dimensional numerical simulation calculation is conducted for the butterfly valve DN50 under the two conditions of 100 and 30% openings. Figure 10 shows the velocity vector distribution at 0.2 m before and after the pipeline when the valve opening is 100 and 30% at different flow velocities. This figure demonstrates that the water flowing through the butterfly valve is obstructed by its central axis plate when the valve is opened at 100%. Therefore, the overflow area of the water body is smaller than that of the pipeline, increasing the flow velocity at the flow passage. The bottom flow velocity of the valve is 0.26 m/s, which is approximately twice the flow velocity of the inlet, under $V = 0.11$ m/s and 100% valve opening. Meanwhile, when $V = 0.183$ m/s and the valve opening is 100%, the bottom flow velocity of the valve is 0.46 m/s, which is approximately 2.56 times the flow velocity of the inlet. When the initial opening of the valve is 30%, the opening of the plate is substantially small at this time and the flow area near the valve is seriously reduced, which leads to the narrowing of the flow passages at both ends of the valve. Consequently, the flow velocity around the flow channel and near the partial area of the pipe wall at the front and rear ends of the valve plate increases and a certain flow velocity gradient is formed, inducing the extremely turbulent internal flow field at the valve plate core. The fluid at the front of the butterfly plate core moves in the direction of the flowing water, while that behind the core moves in the opposite direction to the flowing water and creates a vortex at the top. The flow velocity of the water on the side moving against the direction of the flowing water is larger than that of the water moving in the direction of the flowing water at the bottom of the valve. The areas with the largest flow velocity and the most concentrated streamlines are also most severely impacted by the water flow. The bottom flow velocity of the valve is 0.79 m/s when $V = 0.11$ m/s, and the valve opening is 30%: the bottom flow velocity of the valve is 1.14 m/s, which is 6.23 times the flow velocity of the inlet, under $V = 0.183$ m/s and 30% valve opening. A small valve opening induces a turbulent

flow pattern at the valve and a large flow velocity at the top and bottom of the valve.

The average flow velocities obtained at 100 and 30% valve openings are plotted in Fig. 11. The figure shows that under the six different inlet flow velocities, the average flow velocity of the pipeline at 30% valve opening is larger than that at 100% valve opening, and the average flow velocity at 100% valve opening is slightly larger than the inlet flow velocity. For example, when $V = 0.183$ m/s, the flow velocity of inlet is 0.183 m/s, the average flow velocity at 100% valve opening is 0.191 m/s, and the average flow velocity at 30% valve opening is 0.221 m/s; when $V = 0.284$ m/s, the inlet flow velocity is 0.284 m/s, the average flow velocity at 100% valve opening is 0.292 m/s, and the average flow velocity at 30% valve opening is 0.325 m/s. The experimental results reveal that the direct water hammer pressure generated by the rapid closing of the valve at various valve openings is different. The direct water hammer pressure generated by closing the valve at 30% valve opening exceeds the pressure generated by that at 100% valve opening, and the excess value can reach a maximum of 10%. The above results obtained from a three-dimensional numerical simulation of the flow pattern near the valve at different openings demonstrate that the large water hammer pressure under a small valve opening is due to the turbulent flow pattern at the bottom of the valve. Under six different inlet flow velocities, the maximum flow velocity at the bottom of the valve with 30% opening is approximately three times that with 100% opening, and the average flow velocity at 30% valve opening exceeds that at 100% valve opening by approximately 13%. Therefore, the flow velocity at the bottom of the valve with 30% opening is larger than that at 100% opening. The theory of direct water hammer indicates that the increase in water hammer pressure is related to the change in flow velocity; thus, a considerable change in flow velocity induces a large direct water hammer pressure. The variation in the average flow velocity at 30% valve opening is larger than that at 100% opening by 10%. Therefore, the measured direct water hammer pressure generated by rapidly closing the valve at 30% valve opening is relatively large.

5 Discussion

In this paper, we mainly compare all the results of the experiments with the classical Joukowsky formula. For the viscoelastic Joukowsky head (VJH) formula, during the creep calibration procedure, the creep coefficient of a viscoelastic pipe was determined based on the results collected from transient tests. At the moment, we cannot conduct tests of the creep function to compare the measured results with the VJH formula. In later studies, we will also focus on the applicability of the VJH formula to direct water hammer pressures

Fig. 10 Vector distribution of flow velocity when the valve opening is 100 and 30% at different flow velocities (30 and 100% valve openings are, respectively, shown above and below)
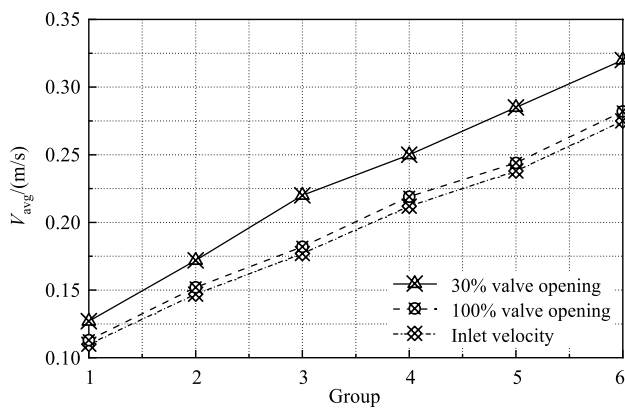

(a) 0.11 m/s

(b) 0.147 m/s

(c) 0.183 m/s

(d) 0.216 m/s

(e) 0.247 m/s

(f) 0.284 m/s
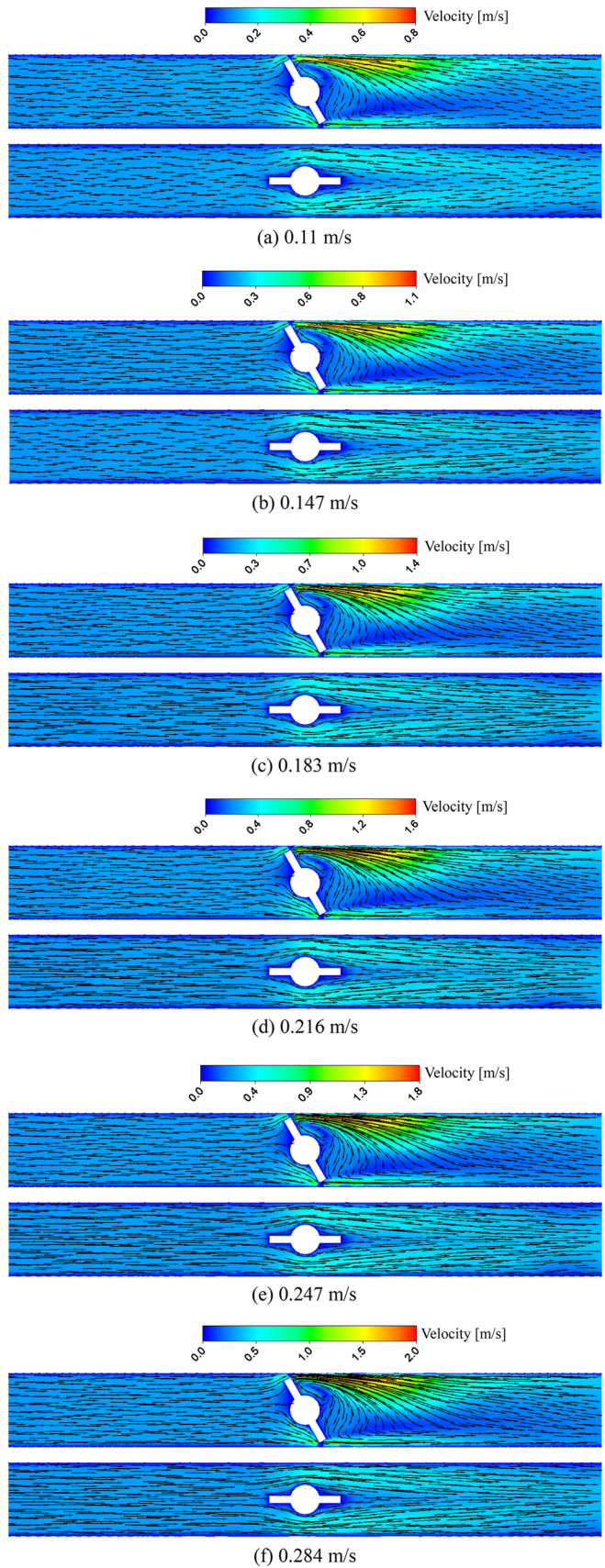
Fig. 11 Comparison of average flow velocities obtained from numerical simulation at different valve openings

generated in different viscoelastic pipes. We believe that all the experimental data in this paper can be used to validate and predict the mathematical model and response of the viscoelastic pipe mechanism. The variation in direct water hammer pressure in PMMA pipes was analyzed. Therefore, the applicability of our findings to other viscoelastic pipes (PVC, PE, HDPE) and how to determine the creep function of PMMA pipes will continue to be studied experimentally. In the numerical simulation on the pipe, we focused on the flow field distribution of constant flow with different initial opening of the valve, without applying the Joukowsky formula to the modeling of viscoelastic pipes, and how the properties of the material and the valve action are correctly applied in the mathematical model is the focus of the next stage of the authors' research.

6 Conclusions

A series of experiments is conducted in this paper on the direct water hammer pressure generated by different valve openings, and the variation law of the direct water hammer pressure in the PMMA pipeline is studied. The conclusions are as follows.

(1) At different flow rates and initial valve openings, the direct water hammer pressure generated by a rapidly closing valve is much greater than the calculated value of the Joukowsky formula, which is due to the time-dependent nature of viscoelastic pipes, i.e., the deformation of the pipe is affected by time, resulting in the inapplicability of the Joukowsky formula for calculating the direct water hammer pressure of viscoelastic pipes. The test results show that the direct water hammer pressure is also related to the valve closing time,

and the shorter valve closing time will lead to a significant increase in direct water hammer pressure.

(2) Under certain flow velocity, the direct water hammer pressure generated by closing the valve at 30% opening exceeds that at 100% opening by a maximum of 10% compared with that generated by closing the valve at 100% and 30% valve openings. Therefore, the direct water hammer pressure in the viscoelastic pipeline is related to the initial opening of the valve. A small valve opening induces a substantial direct water hammer pressure.

(3) The simulation results of the flow field show that the flow pattern of the water body is relatively smooth and the average flow velocity is small under 100% valve opening. Meanwhile, the water flow velocity at both ends of the valve plate is relatively large under 30% valve opening. Thus, the impulse on the wall is strong and the average flow rate is large. A small valve opening induces large flow velocity at the bottom water and high direct water hammer pressure.

References

1. Pan B, Duan HF, Meniconi S et al (2020) Multistage frequency-domain transient-based method for the analysis of viscoelastic parameters of plastic pipes. J Hydraul Eng 146(3):04019068
2. Zhang Y, Liu M, Liu Z et al (2019) Pump-stoppage-induced water hammer in a long-distance pipe: a case from the Yellow River in China. Water Supply 19(1):216–221
3. Ye J, Zeng W, Zhao Z et al (2020) Optimization of pump turbine closing operation to minimize water hammer and pulsating pressures during load rejection. Energies 13(4):1000
4. Firouzi A, Yang W et al (2021) Failure of corrosion affected buried cast iron pipes subject to water hammer. Eng Fail Anal 120:104993
5. Arefi MH, Ghaeini-Hessaroeyeh M et al (2021) Numerical modeling of water hammer in long water transmission pipeline. Appl Water Sci 11:1–10
6. Lupa SI, Gagnon M, Muntean S et al (2022) The impact of water hammer on hydraulic power units. Energies 15(4):1526
7. Tran PD (2017) Pressure transients caused by air-valve closure while filling pipelines. J Hydraul Eng 143(2):04016082
8. Besharat M, Tarinejad R, Ramos HM (2016) The effect of water hammer on a confined air pocket towards flow energy storage system. J Water Supply Res Technol—AQUA 65(2):116–126.
9. Miao D, Zhang J, Chen S et al (2017) Water hammer suppression for long distance water supply systems by combining the air vessel and valve. J Water Supply Res Technol—AQUA 66(5):319–326.
10. Yang L, Li S, Hou YM et al (2007) Improvement of fundamental equation of water hammer. J Hydraul Eng 38(8):948–952

11. Fu Y, Jiang J, Li YH, Ying R (2018) Calculation of pipe water hammer pressure with liquid column separation by improved two-fluid model. Trans Chin Soc Agric Eng 34(15):58–65

12. Wang L, Wang FJ, Huang J, Luo JQ et al (2017) Filling transient analysis in pipelines with air valves. J Hydraul Eng 48(10):1240–1249

13. Chen Y, Gu W, Wang D et al (2021) Experimental study and numerical calculation of water hammer effect of closing valve of ball type regulating valve. J Drain Irrigation Mach Eng 39(10):1027–1032

14. Roberts A, Thomas B, Sewell P et al (2019) Generating renewable power from water hammer pressure surges. Renew Energy 134:1392–1399

15. Wang S, Yu X, Ni W et al (2019) Water hammer protection combined with air vessel and surge tanks in long-distance water supply project. J Drain Irrigation Mach Eng 37(5):406–412

16. Li N, Zhang J, Shi L et al (2020) Water hammer protection characteristic of combined air vessel and overpressure relief valve. J Drain Irrigation Mach Eng 38(3):254–260

17. Zeng W, Yang J, Tang R et al (2016) Extreme water-hammer pressure during one-after-another load shedding in pumped-storage stations. Renew Energy 99:35–44

18. Wang P, Yu J (2020) Numerical simulation of water hammer boundary conditions based on nozzle outflow law. J Drain Irrigation Mach Eng 38(8):814–818, 834

19. Zhang J, Yang S, Yu X et al (2022) Water hammer analytical method considering friction of long headrace tunnel. J Huazhong Univ Sci Technol 50(5):95-101

20. Li X, Zhu M, Tao C (2015) Impacts of type of air valve on water hammer protection in pressurized pipelines. J Drain Irrigation Mach Eng 33(7):599–605

21. Zhang D, Wang H, Liu J, Wang C, Ge J, Zhu Y, Chen X, Hu B (2022) Flow characteristics of oblique submerged impinging jet at various impinging heights. J Mar Sci Eng 10(3):399

22. Hu B, Yao Y, Wang M et al (2023) Flow and performance of the disk cavity of a marine gas turbine at varying nozzle pressure and low rotation speeds: a numerical investigation. Machines 11(1):68

23. Wang C, Chen X, Ge J et al (2023) Internal flow characteristics of high-specific-speed centrifugal pumps with different number of impeller blades under large flow conditions. Machines 11(2):138

24. Wang C, Yao Y, Yang Y et al (2023) Automatic optimization of centrifugal pump for energy conservation and efficiency enhancement based on response surface methodology and computational fluid dynamics. Eng Appl Comp Fluid 17(1):2227686

25. Triki A (2018) Dual-technique-based inline design strategy for water-hammer control in pressurized pipe flow. Acta Mech 229(5):2019–2039

26. Triki A, Fersi M (2018) Further investigation on the water-hammer control branching strategy in pressurized steel-piping systems. Int J Press Vessels Pip 165:135–144

27. Wang WX, Kang YM (1992) Analysis of the dynamic characteristics of liquid flow in viscoelastic pipe line. J Fuxin Mining Institute 2:75–81

28. Zhang T, Lv YZ, Yang ZQ et al (2017) Axial vibration response of the viscoelastic fluid-conveying straight pipe induced by water hammer. J Vibrat Eng 30(2):241–248

29. Bergant A, Hou Q, Keramat A et al (2013) Waterhammer tests in a long PVC pipeline with short steel end sections. J Hydraulic Struct 1(1):24–36

30. Gally M, Güney M, Rieutord E (1979) An investigation of pressure transients in viscoelastic pipes. J Fluids Eng 101(4):495

31. Covas D, Ivan S, Helena R et al (2004) The dynamic effect of pipe-wall viscoelasticity in hydraulic transients. Part I experimental analysis and creep characterization. J Hydraul Res 42(5):517–532.

32. Covas D, Stoianov I, Mano JF et al (2005) The dynamic effect of pipe-wall viscoelasticity in hydraulic transients. Part II model development, calibration and verification. J Hydraul Res 43(1):56–70.

33. Soares AK, Covas DI, Reis LF (2008) Analysis of PVC pipe-wall viscoelasticity during water hammer. J Hydraul Eng 134(9):1389–1394

34. Ghidaoui M (2010) Unsteady friction and visco-elasticity in pipe fluid transients. J Hydraul Res 48(3):354–362

35. Keramat A, Kolahi AG, Ahmadi A (2013) Waterhammer modelling of viscoelastic pipes with a time-dependent Poisson's ratio. J Fluids Struct 43:164–178

36. Keramat A, Tijsseling AS, Hou Q et al (2012) Fluid-structure interaction with pipe-wall viscoelasticity during water hammer. J Fluids Struct 28(1):434–455

37. Keramat A, Fathi-Moghadam M, Zanganeh R et al (2020) Experimental investigation of transients-induced fluid–structure interaction in a pipeline with multiple-axial supports. J Fluids Struct 93:102848

38. Keramat A, Haghighi A (2014) Straightforward transient-based approach for the creep function determination in viscoelastic pipes. J Hydraul Eng 140(12):04014058

39. Meniconi S, Brunone B, Ferrante M et al (2014) Energy dissipation and pressure decay during transients in viscoelastic pipes with an in-line valve. J Fluids Struct 45:235–249

40. Jeon S Y, Yoon J Y, Shin MS (2010) Flow characteristics and performance evaluation of butterfly valves using numerical analysis. Conference Series: Earth and Environmental Science. IOP Publishing, Bristol

41. Zhang Y, Xi Z, Sun L (2022) Numerical investigation of water hammer effect in pipeline of NPP considering two-phase compressible flow. Prog Nucl Energy 150:104287

42. Han Y, Shi W, Xu H et al (2022) Effects of closing times and laws on water hammer in a ball valve pipeline. Water 14(9):1497

43. Duan HF, Che TC, Lee PJ et al (2018) Influence of nonlinear turbulent friction on the system frequency response in transient pipe flow modelling and analysis. J Hydraul Res 56(4):451–463

44. Gong J, Stephens ML, Lambert MF et al (2018) Pressure surge suppression using a metallic-plastic-metallic pipe configuration. J Hydraul Eng 144(6):04018025

45. Urbanowicz K, Duan HF, Bergant A et al (2020) Transient liquid flow in plastic pipes. J Mech Eng 66(2):77–90

46. Pezzinga G, Brunone B (2006) Turbulence, friction and energy dissipation in transient pipe flow. WIT Press, Southampton, UK

47. Bergant A, Hou Q, Keramat A et al (2011) Experimental and numerical analysis of water hammer in a large-scale PVC pipeline apparatus. RET 2(2):2